IEEE Access
Multidisciplinary | Rapid Review | Open Access Journal

Received June 28, 2019, accepted July 13, 2019, date of publication July 16, 2019, date of current version August 5, 2019.

Digital Object Identifier 10.1109/ACCESS.2019.2929301

Commutation Failure Prediction Method Considering Commutation Voltage Distortion and DC Current Variation

QI WANG[1], (Member, IEEE), CHAOMING ZHANG[1], XINGQUAN WU[2], AND YI TANG[1], (Senior Member, IEEE)

[1]School of Electrical Engineering, Southeast University, Nanjing 210096, China
[2]State Grid Jiangsu Electric Power Company Maintenance Branch, Nanjing 211106, China

Corresponding author: Qi Wang (wangqi@seu.edu.cn)

This work was supported in part by the National Key Research and Development Program of China under Grant 2018YFB0904500, in part by the National Natural Science Foundation of China under Grant 51707032, and in part by the Open Fund Project from the National Key Laboratory of Smart Grid Protection and Operation Control under Grant SGNR0000GZJS1808086.

ABSTRACT Commutation failure (CF) at the inverter side is one of the most common failures in the line-commutated converter-based high voltage direct current (LCC-HVDC) system. Effective prediction of CF helps to formulate and implement protection measures timely. Since abnormal commutation voltage and DC current are the main reasons causing CF, these two factors should be fully considered in CF prediction. In this paper, to consider the effect of commutation voltage distortion, the time-domain response of the commutation voltage Fourier coefficient is deduced based on the first-order circuit response. To consider the effect of DC current variation, the time-domain response of the DC current is derived by superimposing its steady-state component and transient component, respectively. Based on these two predictive value, the extinction angle (EA) during the commutation is calculated according to the commutation voltage-time area, and the criterion based on EA is proposed to predict the occurrence of CF. The simulation results of the test system built in the PSCAD/EMTDC demonstrate the effectiveness and validity of this method.

INDEX TERMS Commutation failure, commutation voltage distortion, DC current distortion, first-order circuit response.

I. INTRODUCTION

Line-commutated converter based high voltage direct current (LCC-HVDC) technology has provided promising solutions to overcome the challenge of the inverse distribution of energy resources and load, which has been wildly utilized in long-distance bulk power transmission [1]–[4]. Commutation failure (CF) at the inverter side is a very frequent dynamic event in the HVDC system [5], [6]. The occurrence of CF will lead to a rapid drop of DC transmission power, resulting in power shock to AC system. If the first CF is not handled timely, the continuous CFs may occur at local and adjacent inverter station, which will lead to DC blocking and then cause the wide-range power outage [7]. Effective prediction of CF helps to formulate and implement protection measures timely, and improve the security and stability of the power system [8], [9].

The associate editor coordinating the review of this manuscript and approving it for publication was Padmanabh Thakur.

A considerable number of researches have been carried out in the field of CF analysis. The abnormal commutation voltage and the DC current are considered as the major reasons in causing CF [10]–[12]. Thio *et al.* [13] analyze the relationship between the extinction angle (EA) and the root mean square of the commutation voltage. Further, some scholars propose a method to calculate EA based on the nodal impedance matrix and nodal voltage interaction factor [14]. The above research treats the commutation voltage as a fundamental wave. However, the accuracy of the above methods will be affected under certain faults, for the rapid rise of the DC current will cause transformer saturation, leading to the distortion of commutation voltage [15].

Some scholars analyze the influence of the harmonic amplitude, phase angle, and frequency on commutation process, and then propose the index of harmonic influence coefficient to measure the influence of commutation voltage distortion on CF [16]. But the calculation of this index refers to EA, which cannot be measured before the end

of commutation. That means this method can only be used for post-fault analysis rather than prediction. Authors in [17] propose a dynamic evaluation index based on the simplified harmonic commutation coefficient to measure the risk of CF. This method considers the commutation overlap angle approximately unchanged during the commutation. However, the simplification of this method will inevitably introduce relatively great errors, for the commutation overlap angle may change significantly due to the DC current variation and the commutation voltage distortion. Besides these method, a calculation method of pseudo EA is proposed in [18], which can be used as a direct control variable to realize the real-time EA control and thus mitigate the CF. However, this method has deficiencies in accuracy and applicability in some scenarios, for the commutation voltage is assumed as a pseudo value according to the historical data, and the effect of DC current variation is not considered.

Considering the influence of DC current on commutation process, some scholars deduce and calculate the critical current of CF based on the relationship between commutation voltage distortion and DC current [19]. This method can only be used for post-fault analysis of CF rather than ex ante forecasting, for the lack of commutation voltage prediction.

It can be concluded that lack of effective prediction method of commutation voltage and DC current in the transient process is the prominent problem faced by the existing research on predicting CF. Thus, in this paper, a CF prediction method considering commutation voltage distortion and DC current variation is proposed. The main contributions of this paper are: 1) Solve the difficulty of commutation voltage prediction by deducing the time-domain response of the commutation voltage Fourier coefficient based on the first-order circuit response. 2) Solve the difficulty of DC current prediction by deriving the time-domain response of the DC current consisting of the steady-state component and transient component. The proposed method can be utilized to effectively predict a CF caused by AC system faults according to the measurement information during limited time.

The remaining of this paper is as follows: In Section II, the commutation process, and the influence of commutation voltage distortion as well as the DC current variation on CF is analyzed. In Section III, the commutation voltage prediction method is introduced. In Section IV, the DC current prediction method and the CF criterion are proposed. Case studies and conclusions are presented in Section V and Section VI, respectively.

II. DESCRIPTION OF THE COMMUTATION PROCESS AT THE INVERTER SIDE

The structure of six pulse converter at the inverter side is shown in Fig.1. Six thyristor valves named V_1 to V_6 are triggered in sequence, and the conduction interval of adjacent valve is 60°. e_a, e_b,e_c are equivalent three-phase voltage at the inverter side, L_c is the inductance of AC power supply, I_d and U_d are DC voltage and current respectively.

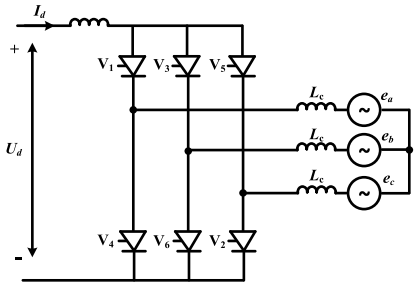

FIGURE 1. Structure of six pulse converter at the inverter side.

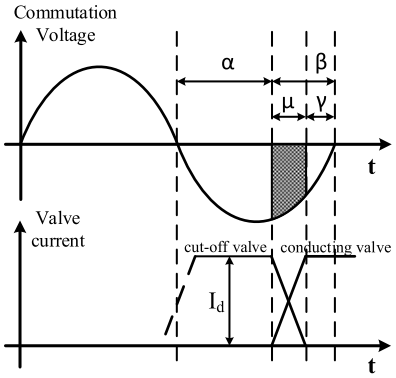

FIGURE 2. The relationship between the commutation voltage and the corresponding valve current during the commutation.

During the commutation, due to the effect of L_c, phase current cannot be changed instantaneously. It takes a certain time for current to transfer from one phase to another, and the electrical angle corresponding to this period is called commutation overlap angle μ. Besides this, the firing angle, leading firing angle, and the extinction angle of valves are generally expressed by α, β, and γ. The relationship between commutation voltage and the corresponding valve current during the commutation is shown in Fig.2.

At the end of commutation, if the expected cut-off valve cannot establish a forward voltage blocking capability, it will conduct again when the commutation voltage cross zero, which is called CF.

Taking the commutation process from valve 1 to valve 3 as an example, the relationship between the commutation voltage e_{ba} and the corresponding valve current i_1, i_3 can be described as:

$$e_{ba} = L_c \frac{di_3}{dt} - L_c \frac{di_1}{dt} \tag{1}$$

For $i_3 = I_d$-i_1, substitute this equation to (1) and integrate the both sides of (1) from t_β to t_γ, then the following equation can be obtained:

$$\int_{t_\beta}^{t_\gamma} e_{ba}(t)dt = \int_{t_\beta}^{t_\gamma} L_c(di_d - 2di_1) \tag{2}$$

where t_β is the time when the commutation begins, and t_γ is the time when the commutation ends.

For $i_1(t_\beta) = I_d(t_\beta)$, and $i_1(t_\gamma) = 0$, thus (2) can be written as:

$$\int_{t_\beta}^{t_\gamma} e_{ba}(t)dt = L_c[I_d(t_\beta) + I_d(t_\gamma)] \tag{3}$$

where $\int_{t_\beta}^{t_\gamma} e_{ba}(t)dt$ is called commutation voltage-time area, corresponding to the shaded area in Fig.2.

Refer to (3), it can be known that t_γ is related to the commutation voltage e_{ba} and the DC current I_d when L_c and t_β are known. The required commutation voltage-time area is determined by I_d, and t_γ is affected by the commutation voltage distortion. Therefore, prediction of the commutation voltage and the DC current is crucial for predicting t_γ, γ, and thus the CF. The prediction process of CF in the $(N+1)$-th cycle can be briefly illustrated by Fig.3.

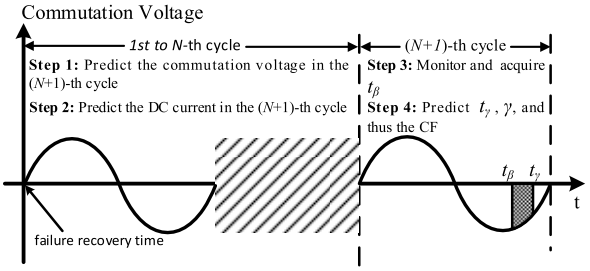

FIGURE 3. The prediction process of CF in the $(N+1)$-th cycle.

Where Step 1, Step 2, and Step 4 mentioned in Fig.3 will be introduced in detail in Section III and Section IV.

III. COMMUTATION VOLTAGE PREDICTION METHOD CONSIDERING DISTORTION

This section is divided into three parts. Firstly, the reason why considers commutation voltage distortion and the elements that need to be predicted are introduced in the Part A. Then the form of transient response in the power system is analyzed in the Part B. Finally, based on the above two parts, the prediction procedures of the commutation voltage are introduced in the Part C.

A. HARMONIC ANALYSIS OF COMMUTATION VOLTAGE

In the HVDC systems, the injection of harmonic mainly comes from the following three aspects [20], [21]: 1) the operation of converter and other power electronic elements in the HVDC systems; 2) the converter transformer saturation caused by the rise of DC current 3) the breaking of the circuit breaker when the system faults.

Set three-phase short circuit fault at the inverter side converter bus in the CIGRE HVDC Benchmark Model. The grounding resistance is 0.01Ω, and the fault time is from 0.5s to 0.6s. The harmonic analysis of the commutation voltage after the fault is shown in Fig.4.

As can be seen in Fig.4, harmonic component of each order increases significantly after the fault. Commutation voltage distortion can affect the commutation voltage-time area, thus

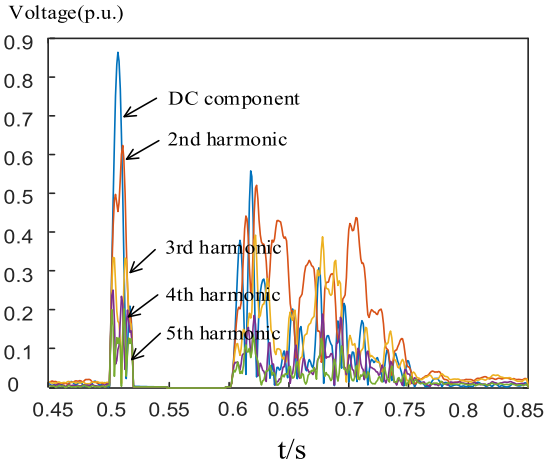

FIGURE 4. Analysis of harmonic component after the fault.

should be considered in the prediction of commutation voltage. Taking e_{ba} as an example, the commutation voltage can be written in the form of Fourier series:

$$e_{ba} = \sum_{n=0}^{\infty} E_n \cos(n\omega_0 t + \varphi_n)dt \tag{4}$$

where $\omega_0 = 100\pi\,(rad/s)$ is the fundamental frequency angular velocity of the system; E_n and φ_n represent the amplitude and phase angle of the n-th harmonic component. Particularly, $n = 0$ represent the DC component and $n = 1$ represent the fundamental frequency component.

Therefore, the prediction of commutation voltage is actually the prediction of E_n and φ_n.

B. ANALYSIS OF THE POWER SYSTEM TRANSIENT RESPONSE

Transient process exists both in failure and recovery for there are energy storage components such as inductance and capacitance in the power system. The HVDC system has long inductive transmission line, thus can be approximately regarded as a first-order *RL* equivalent circuit in the transient process. The transient response of the circuit $f(t)$ corresponds to the solution of the first-order homogeneous differential equation with constant coefficients, which has the following form:

$$f(t) = a(t) + x(t) = a(t) + be^{-t/\tau} \tag{5}$$

where $a(t)$ and $x(t)$ are the steady-state component and transient component of $f(t)$; τ is the eigenvalue of the equivalent circuit; b is a constant related to the parameters and initial conditions of the equivalent circuit.

Denote $T = 2\pi/\omega_0$ as the time of sampling cycle, then the Fourier coefficient A_n and X_n of $a(t)$ and $x(t)$ can be obtained by the following equation:

$$\begin{cases} A_n = \dfrac{1}{T}\int_0^T a(\lambda)e^{-jn\omega_0\lambda}d\lambda \\ X_n = \dfrac{1}{T}\int_0^T x(\lambda)e^{-jn\omega_0\lambda}d\lambda = \dfrac{b}{T}\int_0^T e^{-\lambda/\tau}e^{-jn\omega_0\lambda}d\lambda \end{cases} \tag{6}$$

where j is the unit of imaginary number. Therefore, the Fourier coefficient F_n of $f(t)$ can be obtained:

$$\begin{cases} F_n = A_n + X_n = u_0 e^{jv_0} + u_1 e^{jv_1} \\ u_0 e^{jv_0} = \dfrac{1}{T}\int_0^T a(\lambda) e^{-jn\omega_0\lambda} d\lambda \\ u_1 e^{jv_1} = \dfrac{b}{T}\int_0^T e^{-\lambda/\tau} e^{-jn\omega_0\lambda} d\lambda \end{cases} \tag{7}$$

where u_0, v_0, u_1, v_1 are intermediate variables in the calculation process.

Denote $\tilde{f}_k(t)$ as the k-th sampling cycle, which has the following form:

$$\tilde{f}_k(t) = \{f(t) | t \in [(k-1)T,\ kT]\}, \quad k = 1, 2, 3, \ldots \tag{8}$$

The Fourier coefficient $\tilde{F}_n(k)$ of $\tilde{f}_k(t)$ can be obtained by the following equation:

$$\begin{aligned} \tilde{F}_n(k) = \frac{1}{T}\int_0^T \tilde{f}_k(\lambda) e^{-jn\omega_0\lambda} d\lambda = & \frac{1}{T}\int_0^T a(\lambda + kT) e^{-jn\omega_0\lambda} d\lambda \\ & + \frac{1}{T}\int_0^T x(\lambda + kT) e^{-jn\omega_0\lambda} d\lambda = u_0 e^{jv_0} + u_1 e^{jv_1} \\ & \times e^{(1-k)T/\tau} \end{aligned} \tag{9}$$

In (9), the real part and imaginary part of $\tilde{F}_n(k)$ satisfy the following forms respectively:

$$\begin{cases} real\ (\tilde{F}_n(k)) = \psi'_n(\theta'_n, k) = \mu_0 \cos v_0 + \mu_1 \cos v_1 \\ \qquad\qquad \times e^{(1-k)T/\tau} \\ imag\ (\tilde{F}_n(k)) = \psi''_n(\theta''_n, k) = \mu_0 \sin v_0 + \mu_1 \sin v_1 \\ \qquad\qquad \times e^{(1-k)T/\tau} \end{cases} \tag{10}$$

where ψ'_n and ψ''_n represent the function of $real\ (\tilde{F}_n(k))$ and $imag\ (\tilde{F}_n(k))$ respectively; $\theta'_n = \theta''_n = \theta = \{\tau, \mu_i, v_i | i = 0, 1\}$ represent the parameters related to the system parameters and initial conditions. Refer to (10), if the θ can be obtained, the trends of $\tilde{F}_n(k)$ and then the $\tilde{f}_k(t)$ can be predicted.

It should be noted that θ'_n and θ''_n are generally different due to the existence of data errors, thus θ'_n and θ''_n should be fitted separately in the actual fitting process.

C. PROCEDURES OF COMMUTATION VOLTAGE PREDICTION

When an asymmetric fault occurs in the system, three-phase voltage of the converter bus can be decomposed into positive, negative and zero sequence components [22]. For the existence of rotating elements in the power system, distinct electromagnetic processes will be caused by the passage of different sequence component, so the three-sequence impedance and the equivalent circuit parameters are generally different, which means the three-sequence component should be predicted separately.

Denote the failure recovery time as the initial time, taking the commutation process in the $(N+1)$-th cycle ($N > 2$) as an example, the prediction procedures of commutation voltage are listed as follows:

1) Collect the data of three-phase voltage of the converter bus, and $\tilde{F}_{n(i)}(k)$ can be obtained by Discrete Fourier Transform (DFT), where $i = a, b, c$, $k = 1, 2, \ldots, N$, n represent the harmonic number;

2) Calculate the Fourier coefficients of the three-sequence voltage of the converter bus according to the symmetric component method, and record them as $\tilde{F}_{na(1)}(k)$, $\tilde{F}_{na(2)}(k)$, $\tilde{F}_{na(0)}(k)$ respectively:

$$\begin{bmatrix} \tilde{F}_{na(1)}(k) \\ \tilde{F}_{na(2)}(k) \\ \tilde{F}_{na(0)}(k) \end{bmatrix} = \frac{1}{3}\begin{bmatrix} 1 & \alpha & \alpha^2 \\ 1 & \alpha^2 & \alpha \\ 1 & 1 & 1 \end{bmatrix} \begin{bmatrix} \tilde{F}_{n(a)}(k) \\ \tilde{F}_{n(b)}(k) \\ \tilde{F}_{n(c)}(k) \end{bmatrix} \tag{11}$$

where $k = 1, 2, \ldots, N$, and $\alpha = e^{j\frac{2\pi}{3}} = -0.5 + j0.5\sqrt{3}$;

3) Fit the parameters of ψ'_n and ψ''_n:

$$\begin{cases} \hat{\theta}'_{n(\xi)} = fit(\psi'_n, \{k, real(\tilde{F}_{na(\xi)}(k)) | k = 1, 2, \cdots, N\}) \\ \qquad\qquad\qquad\qquad\qquad\qquad \xi = 1, 2, 0 \\ \hat{\theta}''_{n(\xi)} = fit(\psi''_n, \{k, imag(\tilde{F}_{na(\xi)}(k)) | k = 1, 2, \cdots, N\}), \end{cases} \tag{12}$$

where $\hat{\theta}'_{n(\xi)}$ and $\hat{\theta}''_{n(\xi)}$ represent the fitting parameters of ψ'_n and ψ''_n; fit is the fitting function based on the principle of least square, its form is $\hat{\theta} = fit(fun, \{X, Y\})$, which means fitting $Y = fun(\theta, X)$ and returning the fitting parameters $\hat{\theta}$.

4) Predict $\hat{\tilde{F}}_{na(\xi)}(N+1)$:

$$\begin{aligned} \hat{\tilde{F}}_{na(\xi)}(N+1) &= real(\hat{\tilde{F}}_{na(\xi)}(N+1)) + j \times imag(\hat{\tilde{F}}_{na(\xi)}(N+1)) \\ &= \psi'_n(\hat{\theta'}_{n(\xi)}, N+1) + j\psi''_n(\hat{\theta''}_{n(\xi)}, N+1), \\ &\qquad\qquad \xi = 1, 2, 0 \end{aligned} \tag{13}$$

5) Calculate $\hat{\tilde{F}}_{n(i)}(N+1)$ according to the inverse transformation of symmetric component method, $i = a, b, c$:

$$\begin{bmatrix} \hat{\tilde{F}}_{n(a)}(N+1) \\ \hat{\tilde{F}}_{n(b)}(N+1) \\ \hat{\tilde{F}}_{n(c)}(N+1) \end{bmatrix} = \begin{bmatrix} 1 & 1 & 1 \\ \alpha^2 & \alpha & 1 \\ \alpha & \alpha^2 & 1 \end{bmatrix} \begin{bmatrix} \hat{\tilde{F}}_{na(1)}(N+1) \\ \hat{\tilde{F}}_{na(2)}(N+1) \\ \hat{\tilde{F}}_{na(0)}(N+1) \end{bmatrix} \tag{14}$$

6) Predict the commutation voltage during the commutation in the $(N+1)$-th cycle:

The harmonic coefficient of three-phase voltage can be approximately represented by $\hat{\tilde{F}}_{n(i)}(N+1)$, $i = a, b, c$. Taking the commutation process from valve 1 to valve 3 as an example, the predictive value of E_n and φ_n in (4) can be calculated by the following equation:

$$\begin{cases} \hat{E}_n = \left| \hat{\tilde{F}}_{n(b)}(N+1) - \hat{\tilde{F}}_{n(a)}(N+1) \right| \\ \hat{\varphi}_n = angle\left(\hat{\tilde{F}}_{n(b)}(N+1) - \hat{\tilde{F}}_{n(a)}(N+1) \right) \end{cases} \tag{15}$$

where $\hat{E}_n$ and $\hat{\varphi}_n$ are the predictive value of amplitude and phase angle of the n-th harmonic.

IV. THE DC CURRENT PREDICTION METHOD AND COMMUTATION FAILURE CRITERION

To solve the difficulty of DC current prediction, the time-domain response of the DC current is derived in the Part A.

Then based on the predictive commutation voltage and DC current, the criterion of CF and its prediction method are introduced in the Part B.

A. THE DC CURRENT PREDICTION METHOD IN THE COMMUTATION PROCESS

Taking the commutation process from valve 1 to valve 3 as an example, the equivalent circuit of the commutation process is shown in Fig.5(a) expected the valves in the cut-off state. The equivalent resistance and inductance of the transmission line are represented by R and L; e_{aR}, e_{bR}, e_{cR} and e_{aI}, e_{bI}, e_{cI} are three-phase instantaneous voltage at the rectifier and inverter side; L_c is the inductance of AC power supply. Ignoring the conducting voltage drop of thyristor valves, Fig.5(a) can be simplified as Fig.5(b).

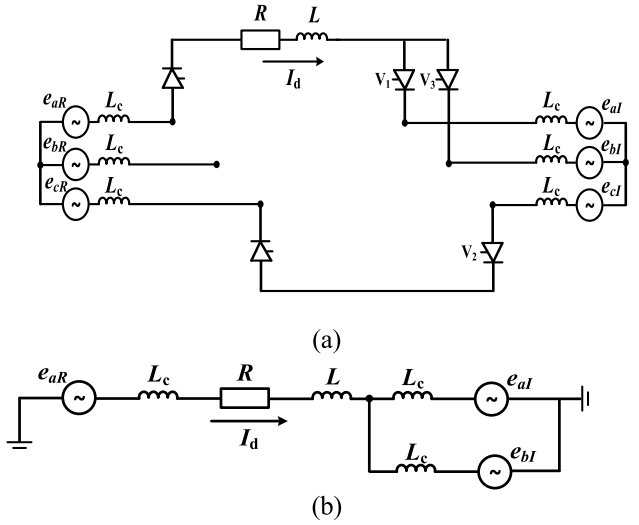

FIGURE 5. The equivalent circuit and the simplified equivalent circuit during the commutation. (a) The equivalent circuit during the commutation; (b) The simplified equivalent circuit during the commutation.

According to the superposition theorem [23], the DC current in the commutation process is composed of steady-state component and transient component. The specific form is shown in Fig.6.

In Fig.6, $\dot{E}_{iRn}$ and $\dot{E}_{iIn}$ represent the n-th harmonic phasor of the rectifier and inverter phase voltage respectively, $i = a, b, c$. $\dot{I}_{dn\_\infty}$ represent the n-th harmonic phasor of the DC current steady-state component. $I_{d\_p}(t)$ represent the DC current transient component, and $I_{d\_p}(0_+)$ is the initial value of $I_{d\_p}(t)$. $\delta(t)$ is the unit impulse function.

The steady-state component of DC current $I_{d\_\infty}(t)$ can be obtained by the following equation:

$$\begin{cases} I_{d\_\infty}(t) = \sum_{n=0}^{\infty} \left|\dot{I}_{dn\_\infty}\right| \cos\left(n\omega_0 t + angle(\dot{I}_{dn\_\infty})\right) \\ \dot{I}_{dn\_\infty} = \dfrac{2\dot{E}_{aRn} - \dot{E}_{aIn} - \dot{E}_{bIn}}{2R + jn\omega_0(2L + 3L_c)} \end{cases} \tag{16}$$

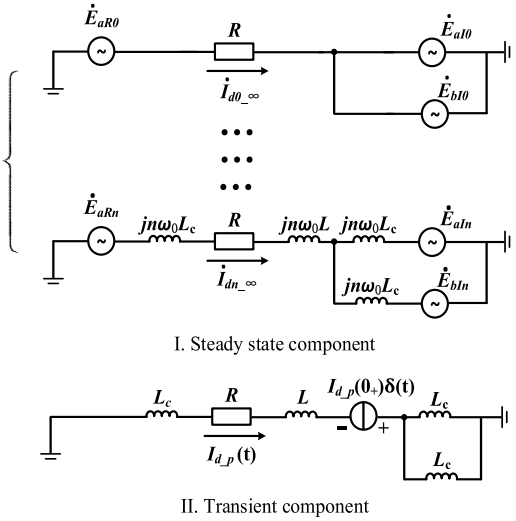

FIGURE 6. The equivalent circuit of steady-state component and transient component of DC current.

The transient component of the DC current $I_{d\_p}(t)$ can be obtained by the following equation:

$$\begin{cases} I_{d\_p}(t) = I_{d\_p}(0_+)e^{-\frac{R}{L+1.5L_c}t} \\ I_{d\_p}(0_+) = I_d(0_+) - I_{d\_\infty}(0_+) \end{cases} \tag{17}$$

where $I_d(0_+)$ and $I_{d\_\infty}(0_+)$ are the initial value of I_d and I_{d_∞}.

The full response of DC current during the commutation consists of DC current steady-state and transient component, which can be written as:

$$I_d(t) = I_{d\_\infty}(t) + I_{d\_p}(t) \tag{18}$$

Combine (16), (17), (18), and substitute the predictive value of the three-phase voltage, then the predictive DC current during the commutation can be obtained by the following equation:

$$\begin{aligned} \hat{I}_d(t) = &\left(I_d(0_+) - \sum_{n=0}^{\infty} \tilde{I}_n \cos\tilde{\varphi}_n\right) e^{-\frac{R}{L+1.5L_c}t} \\ &+ \sum_{n=0}^{\infty} \tilde{I}_n \cos(n\omega_0 t + \tilde{\varphi}_n) \\ \text{where } &\begin{cases} \tilde{I}_n = \left|\dfrac{2\hat{\dot{E}}_{aRn} - \hat{\dot{E}}_{aIn} - \hat{\dot{E}}_{bIn}}{2R + jn\omega_0(2L + 3L_c)}\right| \\ \tilde{\varphi}_n = 2\hat{\varphi}_{aRn} - \hat{\varphi}_{aIn} - \hat{\varphi}_{bIn} - \arctan\left(\dfrac{n\omega_0(L + 1.5L_c)}{R}\right) \end{cases} \end{aligned} \tag{19}$$

In (19), $\hat{\dot{E}}_{iRn}$, $\hat{\varphi}_{iRn}$ represent the phasor and phase angle of the three-phase voltage at the rectifier side, and $\hat{\dot{E}}_{iIn}$, $\hat{\varphi}_{iIn}$ represent the phasor and phase angle of the three-phase voltage at the inverter side; $i = a, b, c$.

B. COMMUTATION FAILURE CRITERION

The essence of predicting CF is to predict EA γ. According to the definition, the predictive value of EA $\hat{\gamma}$ can be expressed by the following equation:

$$\hat{\gamma} = \omega_0(\hat{t}_0 - \hat{t}_\gamma) \tag{20}$$

where $\hat{t}_0$ represent the predictive commutation voltage zero-crossing time; $\hat{t}_\gamma$ represent the predictive time of the end of commutation.

Base on (4), $\hat{t}_0$ can be calculated by the following equation:

$$\begin{cases} \sum_{n=0}^{\infty} \hat{E}_n \cos(n\omega_0 \hat{t}_0 + \hat{\varphi}_n)dt = 0 \\ s.t. \quad \hat{t}_0 \in [t_\beta, t_\beta + \pi] \end{cases} \tag{21}$$

Substitute (15) and (19) into (3), $\hat{t}_\gamma$ can be calculated by the following equation:

$$\int_{t_\beta}^{\hat{t}_\gamma} \sum_{n=0}^{\infty} \hat{E}_n \cos(n\omega_0 t + \hat{\varphi}_n)dt - L_c[I_d(t_\beta) + \hat{I}_d(\hat{t}_\gamma)] = 0 \tag{22}$$

With the increase of harmonic number n, E_n will decay rapidly, thus the influence of high-frequency harmonic can be ignored in (21) and (22). In addition, it is worth mentioning that (21) and (22) belong to the category of transcendental equations, in which the analytic solutions cannot be calculated. This paper will solve this problem by numerical methods.

CF is considered to occur when $\hat{\gamma}$ is less than the limit EA $\gamma_{\min}$. Generally, it takes 400us before the expected cut-off valve can establish a forward voltage blocking capability, and the corresponding electrical angle is 7.2°. Therefore, it is generally considered that $\gamma_{\min}$ equals to 7.2°.

V. CASE STUDY

This section is to verify the validity of the proposed method. In the Part A, the parameters and fault settings of the test system is introduced. And the simulation results are presented and analyzed in the Part B, which show the effectivity of this CF prediction method.

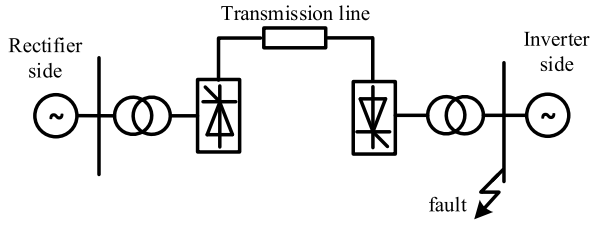

FIGURE 7. The structure of CIGRE HVDC Benchmarking model.

A. INTRODUCTION OF TEST SYSTEM

The CIGRE HVDC Benchmark Model (Fig.7) is applied in this paper. This model is built in PSCAD/EMTDC, the rated voltage and capacity of DC side is 500kV and 1000MW, respectively.

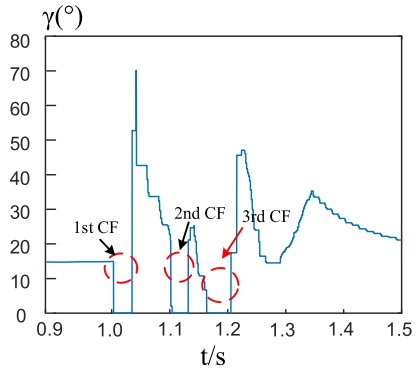

FIGURE 8. Curve of EA during the failure.

The three-phase short circuit fault is set at the converter bus of the inverter side with grounding resistance of 20 Ω. Failure duration is 0.1s, from 1.0s to 1.1s. The curve of EA during the failure is shown in Fig.8.

It can be seen from Fig.8 that the first CF occurs at 1.00285s, and then two continuous CFs occur at 1.02150s and 1.64160s respectively. Following is mainly the analysis of the third CF.

B. SIMULATION RESULTS

1) PREDICTION OF THE COMMUTATION VOLTAGE

Set simulation step as 50us, thus the sampling frequency f_s equals to 20kHz. In this section, the three-sequence components of commutation voltage in the 4th to 8th cycles are predicted.

Taking the fundamental frequency (50Hz) and double fundamental frequency (100Hz) harmonic components as examples, the comparison of predictive and actual value is shown in Fig.9.

The three-sequence harmonic components are divided into real part and imaginary part respectively for analysis. The blue dot means the actual value, and the predictive curve is obtained by fitting the previous N-1 actual value, and used for predicting the N-th actual value.

As Fig.8 shows, the prediction error decrease gradually with the increase of N, which means that more fitting data can help to improve the accuracy of parameters. Further analysis shows that the positive-sequence component is the largest in the three-sequence component. And because of the Y-Δ connection mode of the converter transformer, there is no zero-sequence current in the secondary side, so the zero-sequence component is almost zero. Except the positive-sequence component of fundamental frequency, the other components gradually decay to zero.

Convert the three-sequence component into three-phase component, the comparison of predictive and actual value is shown in Table 1.

Denote $Error_N$ as the prediction error of the commutation voltage in the N-th cycle:

$$Error_N = \left| (V_{Nb}e^{j\varphi_{Nb}} - V_{Na}e^{j\varphi_{Na}}) - (\tilde{V}_{Nb}e^{j\tilde{\varphi}_{Nb}} - \tilde{V}_{Na}e^{j\tilde{\varphi}_{Na}}) \right| \tag{23}$$

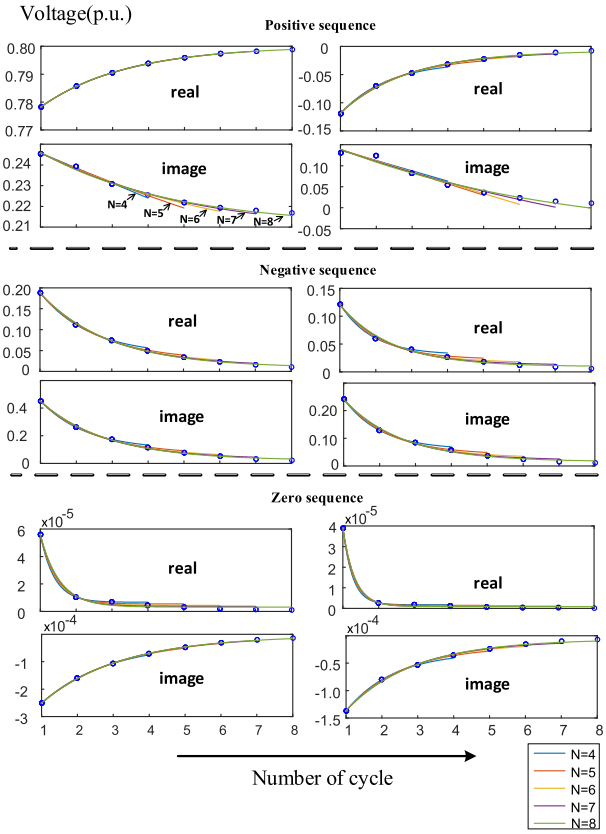

FIGURE 9. Comparison of the predictive and actual three-sequence harmonic components in the 4th to 8th cycles.

The comparison of $Error_N$ in the 4th to 8th cycles is shown in Table 2.

It can be seen from Table 2 that $Error_N$ of the fundamental frequency (50Hz) and double fundamental frequency (100Hz) are all relatively small, and show a decreasing trend in general. It shows that this proposed method can effectively predict the commutation voltage after failure recovery.

2) PREDICTION OF DC CURRENT

Based on (19), the DC current can be predicted according to the predictive three-phase voltage. Taking the commutation process from valve 1 to valve 3 in the 4th cycle as an example, compare the predictive and real curve of the DC current in the commutation process, and the result is shown in Fig.10.

It can be seen in Fig.10 that the actual DC current approximately rise by 0.032kA during the commutation. The prediction error of the DC current at the end of commutation is about 0.001kA, which is much smaller than the changed value. Therefore, the DC current prediction method proposed in this paper has relatively high prediction accuracy.

3) PREDICTION OF COMMUTATION FAILURE

This section gives the prediction results of CF and analyze the influence of commutation voltage distortion and DC current variation on the prediction accuracy of EA.

TABLE 1. Comparison of predictive and actual three-phase components in the 4th to 8th cycles.

(a) f=50Hz

N	i	V_{Ni}	$\tilde{V}_{Ni}$	φ_{Ni}	$\tilde{\varphi}_{Ni}$
4	a	0.8332	0.8339	0.2884	0.2902
	b	0.8297	0.8298	-1.8318	-1.8340
	c	0.8128	0.8103	2.3737	2.3741
5	a	0.8316	0.8321	0.2796	0.2811
	b	0.8293	0.8294	-1.8320	-1.8338
	c	0.8180	0.8159	2.3679	2.3682
6	a	0.8305	0.8310	0.2737	0.2750
	b	0.8290	0.8290	-1.8321	-1.8337
	c	0.8215	0.8197	2.3641	2.3644
7	a	0.8299	0.8303	0.2698	0.2709
	b	0.8288	0.8288	-1.8322	-1.8335
	c	0.8238	0.8223	2.3616	2.3618
8	a	0.8294	0.8298	0.2672	0.2682
	b	0.8286	0.8287	-1.8322	-1.8334
	c	0.8254	0.8241	2.3599	2.3602

(b) f=100Hz

N	i	V_{Ni}	$\tilde{V}_{Ni}$	φ_{Ni}	$\tilde{\varphi}_{Ni}$
4	a	0.1112	0.1181	1.6171	1.5328
	b	0.0044	0.0212	-1.4342	-2.8770
	c	0.1069	0.1137	-1.5282	-1.4295
5	a	0.0737	0.0720	1.6233	1.4249
	b	0.0021	0.0293	-1.3186	-3.0253
	c	0.0717	0.0705	-1.5240	-1.3034
6	a	0.0487	0.0502	1.6327	1.4046
	b	0.0006	0.0226	-0.7551	-3.0634
	c	0.0483	0.0499	-1.5179	-1.2818
7	a	0.0322	0.0348	1.6471	1.3628
	b	0.0007	0.0185	0.9567	-3.1047
	c	0.0328	0.0353	-1.5089	-1.2436
8	a	0.0212	0.0243	1.6690	1.3000
	b	0.0014	0.0156	1.2698	3.1405
	c	0.0225	0.0251	-1.4961	-1.1993

where V_{Ni}, $\tilde{V}_{Ni}$ and φ_{Ni}, $\tilde{\varphi}_{Ni}$ are the predictive and actual value of voltage amplitude (p.u.) and phase angle (rad) in the N-th cycle.

TABLE 2. Comparison of $error_N$ in the 4th to 8th cycles.

Harmonic frequency	N				
	4	5	6	7	8
50Hz	0.0024	0.0019	0.0017	0.0014	0.0014
100Hz	0.0318	0.0440	0.0344	0.0287	0.0249

The commutation voltage and conducting current of valve 1 in the 4th cycle is shown in Fig.11.

It can be seen from Fig.11 that when the commutation voltage cross zero, the conducting current of valve 1 has not dropped to zero, leading to the CF. According to the method proposed in this paper, the EA of valve 1 during this commutation is predicted below.

For comparison, four prediction methods considering different factors are adopted:

I: Both the commutation voltage distortion and DC current variation are considered, which is the proposed method in this paper;

II: Only the commutation voltage distortion is considered;

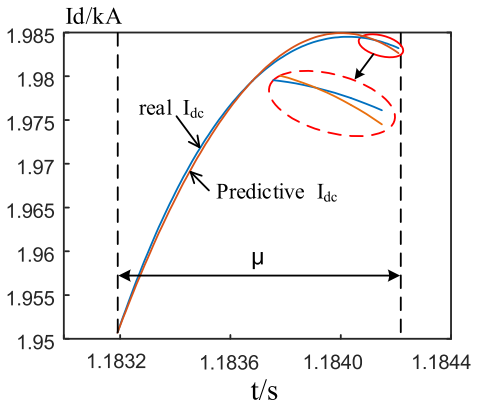

FIGURE 10. Comparison of the predictive and actual curve of the DC current during the commutation in the 4th cycle.

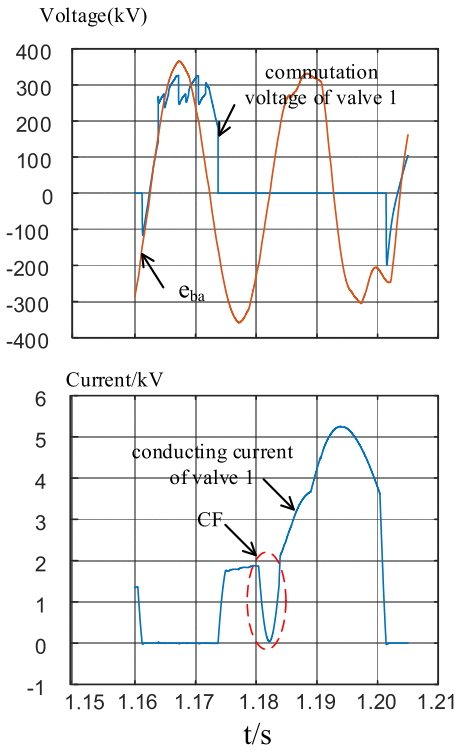

FIGURE 11. Commutation voltage and conducting current of valve 1 in the 4th cycle.

III: Only the DC current variation is considered;

IV: Traditional method without considering the commutation voltage distortion and DC current variation is adopted.

The comparison of the actual and predictive EA of the four methods is shown in Table 3.

For the sampling frequency f_s equals to 20kHz, thus the minimum error of the predictive EA is 0.9°. It can be seen from Table 3 that the prediction accuracy of EA can be effectively improved by considering S1 and S2, especially the S1.

In actual operation, the control strategy of Constant Extinction Angle (CEA) is adopted at the inverter side. The signal used for CEA is the minimum EA of six valves in one cycle, which is denoted as min_γ in this paper. The actual and predictive min_γ of the four methods in the failure are shown in Fig.12.

TABLE 3. Comparison of actual and predictive extinction angle of the four methods.

	$\hat{t}_0$ (s)	$\hat{t}_\gamma$ (s)	$\hat{\gamma}$ (°)
Real data	1.18225	/	/
Method I	1.18210	1.18190	3.6
Method II	1.18210	1.18185	4.5
Method III	1.20505	1.20430	13.5
Method IV	1.17000	1.16920	14.4

where $\hat{t}_0$, $\hat{t}_\gamma$, and $\hat{\gamma}$ are the predictive commutation voltage zero-crossing time; commutation end time, and EA respectively.

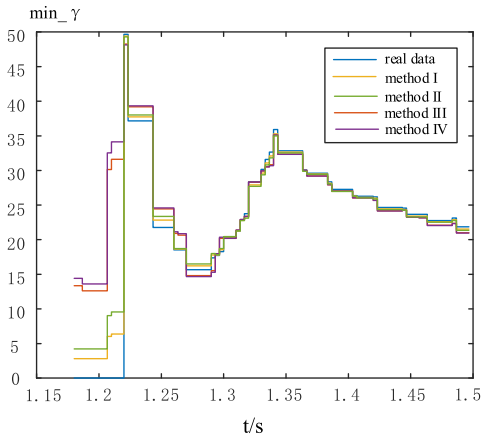

FIGURE 12. Commutation of actual and predictive min_γ of the four methods in the failure.

As can be seen in Fig.12, the predictive min_γ of the four methods deviate greatly in the early stage of the failure recovery. In this stage, Method I and Method II can effectively predict the CF, and Method I performs better. In the late stage of the failure recovery, the predictive min_γ of the four methods are all closed to the actual value. The reason is that in the late stage of failure recovery, the distortion of the commutation voltage has been alleviated, and the DC current variation is relatively small, which have less influence on EA.

VI. CONCLUSION

The factors related to the commutation process are analyzed from the mechanism of CF in this paper, and in view of this, a method to predict CF considering commutation voltage distortion and DC current variation is proposed. By analyzing the simulation results of the CIGRE HVDC Benchmarking Model built in PSCAD/EMTDC, it can be concluded that:

1) The predictive commutation voltage based on the first-order circuit response is in good agreement with the actual value, which means the commutation voltage can be effectively predicted by the proposed method.

2) By comparing with the actual value, it shows that the derived time-domain response of the DC current consisting of steady-state component and transient component can effectively reflect the change of DC current during the commutation.

3) The prediction accuracy of EA can be effectively improved by considering the commutation voltage distortion and DC current variation, especially the former.

The above results show the validity of the proposed method in predicting CF. Further working will consider the effect of capacitance on the form of circuit transient response, which can improve the adaptability of the proposed method in more complex system.

REFERENCES

[1] J. Wu, H. Li, G. Wang, and Y. Liang, "An improved traveling-wave protection scheme for LCC-HVDC transmission lines," *IEEE Trans. Power Del.*, vol. 32, no. 1, pp. 106–116, Feb. 2017.

[2] Y. Xue and X.-P. Zhang, "Reactive power and AC voltage control of LCC HVDC system with controllable capacitors," *IEEE Trans. Power Syst.*, vol. 32, no. 1, pp. 753–764, Jan. 2017.

[3] K. Rouzbehi, S. S. H. Yazdi, and N. S. Shariati, "Power flow control in multi-terminal HVDC grids using a serial-parallel DC power flow controller," *IEEE Access*, vol. 6, pp. 56934–56944, 2018.

[4] G. Zou, Q. Huang, S. Song, B. Tong, and H. Gao, *Novel Transient-Energy-Based Directional Pilot Protection Method for HVDC Line*, vol. 2, no. 1. Henan, China: Protection and Control of Modern Power Systems, 2017.

[5] G. Zhang, L. Jing, M. Liu, B. Wang, and X. Dong, "An improved continuous commutation failure mitigation method in high voltage direct current transmission system," in *Proc. China Int. Conf. Electr. Distrib.*, Tianjin, China, 2018, pp. 1132–1136.

[6] E. Rahimi, A. M. Gole, J. B. Davies, I. T. Fernando, and K. L. Kent, "Commutation failure analysis in multi-Infeed HVDC systems," *IEEE Trans. Power Del.*, vol. 26, no. 1, pp. 378–384, Jan. 2011.

[7] X. Chen, A. M. Gole, and M. Han, "Analysis of mixed inverter/rectifier multi-infeed HVDC systems," *IEEE Trans. Power Del.*, vol. 27, no. 3, pp. 1565–1573, Jul. 2012.

[8] S. Mirsaeidi, X. Dong, D. Tzelepis, D. M. Said, A. Dysko, and C. Booth, "A predictive control strategy for mitigation of commutation failure in LCC-Based HVDC systems," *IEEE Trans. Power Electron.*, vol. 34, no. 1, pp. 160–172, Jan. 2018.

[9] A. Zheng, C. Guo, P. Cui, W. Jiang, and C. Zhao, "Comparative study on small-signal stability of LCC-HVDC system with different control strategies at the inverter station," *IEEE Access*, vol. 7, pp. 34946–34953, 2019.

[10] Y. Ma, H. Li, and G. Wang, "Commutation failures caused by DC line faults in double-circuit LCC-HVDC transmission lines," in *Proc. Int. Conf. Power Syst. Technol.*, Guangzhou, China, 2019, pp. 2725–2732.

[11] Y. Z. Sun, L. Peng, F. Ma, G. J. Li, and P. F. Lv, "Design a fuzzy controller to minimize the effect of HVDC commutation failure on power system," *IEEE Trans. Power Syst.*, vol. 23, no. 1, pp. 100–107, Feb. 2008.

[12] H.-I. Son and H.-M. Kim, "An algorithm for effective mitigation of commutation failure in high-voltage direct-current systems," *IEEE Trans. Power Del.*, vol. 31, no. 4, pp. 1437–1446, Aug. 2016.

[13] C. V. Thio, J. B. Davies, and K. L. Kent, "Commutation failures in HVDC transmission systems," *IEEE Trans. Power Del.*, vol. 11, no. 2, pp. 946–953, Apr. 1996.

[14] G. Li, S. Zhang, T. Jiang, H. Chen, and X. Li, "A method of predicting commutation failure in multi-infeed HVDC systems based on critical failure impedance boundary," in *Proc. IEEE Power Energy Soc. Gen. Meeting*, Chicago, IL, USA, Jul. 2017, pp. 1–5.

[15] J. A. Patel, R. S. Mehta, S. B. Rathod, K. J. Patel, V. N. Rajput, and K. S. Pandya, "Analysis of geomagnetically induced current in transformer," in *Proc. Int. Conf. Elect. Electron. Optim. Techn.*, Chennai, India, Mar. 2016, pp. 3909–3912.

[16] F. Wang, T.-Q. Liu, and X.-Y. Li, "Decreasing the frequency of HVDC commutation failures caused by harmonics," *IET Power Electron.*, vol. 10, no. 2, pp. 215–221, Apr. 2016.

[17] S. Shao, Z. Huang, and Z. Li, "Evaluation of dynamic influence of harmonics of AC system on HVDC commutation failure," in *Proc. Int. Conf. Power Syst. Technol.*, Guangzhou, China, Nov. 2019, pp. 2549–2556.

[18] L. Liu, S. Lin, P. Sun, K. Liao, X. Li, Y. Deng, and Z. He, "A calculation method of pseudo extinction angle for commutation failure mitigation in HVDC," *IEEE Trans. Power Del.*, vol. 34, no. 2, pp. 777–779, Apr. 2019.

[19] W. Ling, W. Jun, Y. Ze, K. Weibo, and L. Yanan, "Analysis of the influence of harmonic on commutation failure of thyristor inverter," in *Proc. IEEE 8th Int. Power Electron. Motion Control Conf.*, Hefei, China, May 2016, pp. 1296–1301.

[20] Y. Li, L. Luo, C. Rehtanz, D. Yang, S. Rüberg, and F. Liu, "Harmonic transfer characteristics of a new HVDC system based on an inductive filtering method," *IEEE Trans. Power Electron.*, vol. 27, no. 5, pp. 2273–2283, May 2012.

[21] K. Yamashita, Y. Kameda, and S. Nishikata, "A harmonics elimination method using a three-winding transformer for HVDC transmission systems," *IEEE Trans. Ind. Appl.*, vol. 54, no. 2, pp. 1645–1651, Nov. 2017.

[22] X.-P. Zhang and H. Chen, "Asymmetrical three-phase load-flow study based on symmetrical component theory," *IEE Proc.-Gener. Transmiss. Distrib.*, vol. 141, no. 3, pp. 248–252, May 1994.

[23] R. Lu and A. Lu, "Applications of the superposition theorem to nonlinear resistive circuits," in *Proc. IEEE Asia–Pacific Conf. Circuits Syst.*, Singapore, Dec. 2016, pp. 1333–1336.

QI WANG (S'13–M'17) received the bachelor's, master's, and Ph.D. degrees in electrical engineering from Southeast University, Nanjing, China, in 2011, 2013, and 2017, respectively.

He is currently a Lecturer with the School of Electrical Engineering, Southeast University. His research interests include power system stability and control, and cyber physical power systems.

CHAOMING ZHANG received the bachelor's degree from Southeast University, Nanjing, China, in 2017, where he is currently pursuing the M.S. degree.

His current research interests include power system operation and control, and HVDC system stability analysis.

XINGQUAN WU received the bachelor's and master's degrees from Southeast University, Nanjing, China, in 2011 and 2014, respectively.

He is currently an Engineer with State Grid Jiangsu Electric Power Company Maintenance Branch. His current research interest includes HVDC technologies.

YI TANG (M'07–SM'19) received the Ph.D. degree from the Harbin Institute of Technology, Harbin, China, in 2006.

He is currently a Professor with Southeast University, Nanjing, China. His research interests include smart grid, power system security, power system stability analysis, renewable energy systems, and cyber physical systems.